Progress in PHOTOVOLTAICS

PROGRESS IN PHOTOVOLTAICS: RESEARCH AND APPLICATIONS
Prog. Photovolt: Res. Appl. 2015; **23**:112–118
Published online 6 August 2013 in Wiley Online Library (wileyonlinelibrary.com). DOI: 10.1002/pip.2405

SHORT COMMUNICATION

Electronic structure of $Ge_{1-x-y}Si_xSn_y$ ternary alloys for multijunction solar cells

Cecilia I. Ventura[1,2]*, Jose D. Querales Flores[1,3], Javier D. Fuhr[1,3] and Rafael A. Barrio[4]

[1] Centro Atómico Bariloche, 8400 Bariloche, Argentina
[2] Universidad Nacional de Río Negro, 8400 Bariloche, Argentina
[3] Instituto Balseiro, 8400-Bariloche, Argentina
[4] Instituto de Física, Univ. Nacional Autónoma de México, Ap. Postal 20–364, 01000 México D.F., Mexico

ABSTRACT

Ternary group-IV alloys have a wide potential for applications in infrared devices and optoelectronics. In connection with photovoltaic applications, they are among the most promising materials for inclusion in the next generation of high-efficiency multijunction solar cells, because they can be lattice matched to substrates as GaAs and Ge, offering the possibility of a range of band gaps complementary to III–V semiconductors. Apart from the full decoupling of lattice and band structures in $Ge_{1-x-y}Si_xSn_y$ alloys, experimentally confirmed, they allow preparation in a controllable and large range of compositions, thus enabling to tune their band gap. Recently, optical experiments on ternary alloy-based films, photodetectors measured the direct absorption edges and probed the compositional dependence of the direct gap. The nature of the fundamental gap of $Ge_{1-x-y}Si_xSn_y$ alloys is still unknown, as neither experimental data on the indirect edges nor electronic structure calculations are available, as yet. Here, we report a first calculation of the electronic structure of $Ge_{1-x-y}Si_xSn_y$ ternary alloys, employing a combined tight-binding and virtual crystal approximation method, which proved to be useful to describe group-IV semiconductor binary alloys. Our results confirm predictions and experimental indications that a 1 eV band gap is indeed attainable with these ternary alloys, as required for the fourth layer plan to be added to present-day record-efficiency triple-junction solar cells, to further increase their efficiency, for example, for satellite applications. When lattice matched to Ge, we find that $Ge_{1-x-y}Si_xSn_y$ ternary alloys have an indirect gap with a compositional dependence reflecting the presence of two competing minima in the conduction band. Copyright © 2013 John Wiley & Sons, Ltd.

KEYWORDS
semiconductor alloys; electronic structure; multijunction solar cells

***Correspondence**
Cecilia I. Ventura, Centro Atómico Bariloche, 8400 Bariloche, Argentina.
E-mail: ventura@cab.cnea.gov.ar

Received 19 October 2012; Revised 10 June 2013; Accepted 23 June 2013

Major advances in epitaxial growth techniques have contributed to an improved understanding of the properties of group III–VI materials and their alloys [1–3]. Modern semiconductor technology requires materials with a precise prescription of both lattice parameter and band gap, which has motivated the study of ternary and quaternary alloys in order to be able to tune them independently [1–4].

The most efficient solar cells currently in production use lattice-matched Ge/GaAs/GaInP triple-junctions grown on bulk Ge substrates. Although these architectures can achieve 39% efficiency by using solar concentrators (at 500 suns) [5], incorporating a fourth junction could provide further improvements in efficiency [4]. The material in this fourth junction should ideally be lattice matched to Ge and have a band gap of ∼1 eV. However, prior to recent advances that make it possible to grow device-quality Ge, GeSn, and GeSiSn alloys on Si substrates, there had been no materials reasonably suitable to meet these requirements [1,6–11]. The emergence of the $Ge_{1-x-y}Sn_xSi_y$ alloys provides the opportunity to incorporate them as a fourth junction in solar cells, taking advantage of the possibility of widely adjustable band gaps at a fixed lattice parameter identical to that of Ge. These materials can also be grown directly, at low cost, on large wafer size Si platforms [9,12]. Experimental results have shown a full decoupling of lattice constant and band structure for $Ge_{1-x-y}Sn_xSi_y$ [8,9] alloys and have suggested that the Ge lattice-matched alloys might have a tunable band gap over the 0.8–1.4 eV range [9]. Recently, the fabrication of working prototype devices on group-IV platforms was reported [12]. In particular, GeSiSn photodiodes on Ge(100) substrates compatible with current multijunction solar cell architectures were produced, as well as similar devices on Si(100) substrates. The latter exhibit inferior crystal quality, induced by the lattice mismatch, but if their photovoltaic performance could be improved, huge cost reductions would ensue. Optical responsivity measurements confirmed [12,13] that defect-free ternary $Ge_{1-x-y}Sn_xSi_y$ alloys lattice matched to Ge(001) substrates possess direct absorption edges between 0.88 and 0.98 eV for small Si ($x \leq 0.2$) and Sn ($y \leq 0.05$) concentrations. The compositional dependence of the direct gap was then derived, indicating important (and compositional dependent) bowing effects. Notwithstanding the large atomic size differences between the components of the ternary alloy, no dramatic deterioration of the I–V or optical characteristics of the diodes was found when the total doping into Ge was increased, at those small Si and Sn concentration ranges, indicating that SiGeSn is behaving like a conventional alloy and can be incorporated into working devices [13]. Quantum efficiency measurements yield values of at least 76% in the devices grown on Ge [12].

In this paper, we report our electronic structure calculation for $Ge_{1-x-y}Si_xSn_y$ ternary alloys. We used a combined tight-binding (TB) and virtual crystal approximation (VCA) approach, originally introduced for group-IV bulk pure elements and binary alloys by Jenkins and Dow [14], which we extended here in order to describe the ternary alloys. Basically, we consider the ternary system as an "effective binary alloy": one component corresponding to Ge , and the second corresponding to a binary Si-Sn alloy. Here, we report the electronic structure results obtained in our TB + VCA approach for the concentration ranges relevant for the envisaged applications in solar cells [9], such that the lattice parameter of the ternary alloy equals that of pure Ge, in order to avoid residual tension/strain effects. The compositional formula for the ternary alloy lattice matched to Ge is $Ge_{1-Z}(Si_\beta Sn_{1-\beta})_Z$, with $\beta = 0.79$ [9].

The TB calculations for electronic band structures are useful because, besides their simplicity, many features can be incorporated by suitably choosing the TB parameters. When applied to Ge, these methods proved not to be straightforward, because a naive calculation considering only sp^3 orbitals does not reproduce essential features such as the indirect band gap and the bandwidths. This arises from the mixing of d electrons in the conduction bands of Ge, which for Si or C are not important, whereas for Sn and Pb are responsible for their metallic behavior. The role of d electrons could be mimicked by introducing a pseudo-orbital s*, without increasing the size of the TB Hamiltonian. Finer properties, such as the exciton spectrum of Ge cannot be explained without introducing spin–orbit interactions. It is well-known that the TB + VCA approach gives excellent predictions for many substitutional binary semiconductor alloys [15,16], in particular for the electronic structure in the energy range around the band gap. In 1984, Newman and Dow[16], presented a complete TB model consisting of an sp^3s^* orbital basis for the binary $Ge_{1-y}Si_y$ alloy, using a simple VCA [17], which provides an excellent description of the electronic structure of this binary alloy, which smoothly evolves between the limiting cases corresponding to the pure components as a function of alloy concentration. In 1987, Jenkins and Dow [14] presented a complete TB model for the binary $Ge_{1-y}Sn_y$ substitutional alloy, including spin–orbit[18], s* orbitals, and second-neighbor interactions[19], and examined several properties of the binary alloy by using VCA.

In our extension of the TB + VCA approach of Jenkins and Dow [14] for the $Ge_{1-x-y}Si_xSn_y$ ternary alloys, we will use the same 20-orbital TB basis (s, p, s* states) they had introduced for the group IV elements, including second-neighbor [14,18] and also spin–orbit interactions [14,16]. Thus, we consider the following averages for the TB + VCA Hamiltonian matrix of the ternary alloy:

$$\begin{aligned} H_{ii} &= (1-x-y)\,[\mathrm{Ge}] + x\,[\mathrm{Si}] + y\,[\mathrm{Sn}]; \\ H_{ij} &= \Big[(1-x-y)[\mathrm{Ge}]\{a_{\mathrm{Ge}}\}^2 + x[\mathrm{Si}]\{a_{\mathrm{Si}}\}^2 \\ &\quad + y\,[\mathrm{Sn}]\,\{a_{\mathrm{Sn}}\}^2\Big]\ \{a(x,y)\}^{-2} \end{aligned} \tag{1}$$

where H_{ii} and H_{ij}, respectively, denote the diagonal and non-diagonal matrix elements of the Hamiltonian, and subindices i and j refer to the TB-orbital states. By [Ge], [Sn], and [Si], we refer to the TB Hamiltonian parameters for Ge and Sn, which are given in Ref. [14], whereas for Si are those given in Ref. [19]. The lattice parameters for pure Ge, Sn, and Si, respectively, are as follows: $a_{\mathrm{Ge}} = 5.65$ Å, $a_{\mathrm{Sn}} = 6.46$Å, and $a_{\mathrm{Si}} = 5.43$Å [20], and we are assuming that Vegard's law[21] is valid for the lattice parameter of the ternary alloy, $a(x, y) = (1-x-y)a_{Ge} + xa_{Si} + ya_{Sn}$.

In Figure 1, we exhibit the TB + VCA band structure obtained for each of the two "effective binary alloy" components, which form the lattice-matched ternary alloy, pure Ge, and $Si_\beta Sn_{1-\beta}$ alloy with $\beta = 0.79$. Ge is seen to exhibit an indirect gap (0.7 eV, i.e., close to the experimental value of 0.67 eV at 300 K [20]) determined by the maximum of the valence band at Γ, the Brillouin zone center of the face-centered cubic diamond lattice, and the minimum of the conduction band located at L. Notice that $Si_{0.79}Sn_{0.21}$ also possesses an indirect gap (0.87 eV) determined by the maximum of the valence band at Γ and the minimum of the conduction band here located near X (as in pure Si). Meanwhile, for $Si_{0.79}Sn_{0.21}$ in TB + VCA, we obtain for the direct gap (at Γ): $E_0 = 2.98$ eV, slightly smaller than the expected value of 3.15 eV obtained, if one uses a linear interpolation between the pure Si (4.1) and α-Sn (–0.4 eV) direct gap values [9].

Figure 2 exhibits the electronic structure we obtained in TB + VCA for the $Ge_{1-Z}(Si_\beta Sn_{1-\beta})_Z$ ternary alloys lattice matched to Ge ($\beta = 0.79$)[9] and amplified around the gap region. We plotted the band structure obtained for

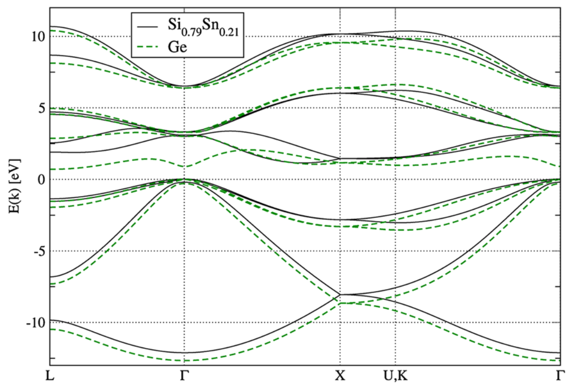

Figure 1. Tight-binding and virtual crystal approximation band structure $E(\vec{k})$ for $Si_{0.79}Sn_{0.21}$ and pure Ge, along with the relevant Brillouin zone paths of the face-centered cubic diamond lattice. Brillouin zone symmetry points: $\Gamma = (0, 0, 0)$, $L = (2\pi/a)(1/2, 1/2, 1/2)$, $X = (2\pi/a)(1, 0, 0)$, $U = (2\pi/a)(1, 1/4, 1/4)$, and $K = (2\pi/a)(3/4, 3/4, 0)$, being a the lattice parameter.

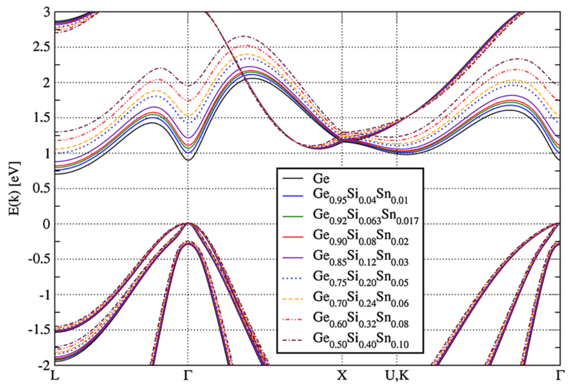

Figure 2. Tight-binding and virtual crystal approximation band structure for ternary alloys lattice matched to Ge: $Ge_{1-Z}(Si_{0.79}Sn_{0.21})_Z$, shown amplified near the gap. Alloy concentrations as indicated in the figure.

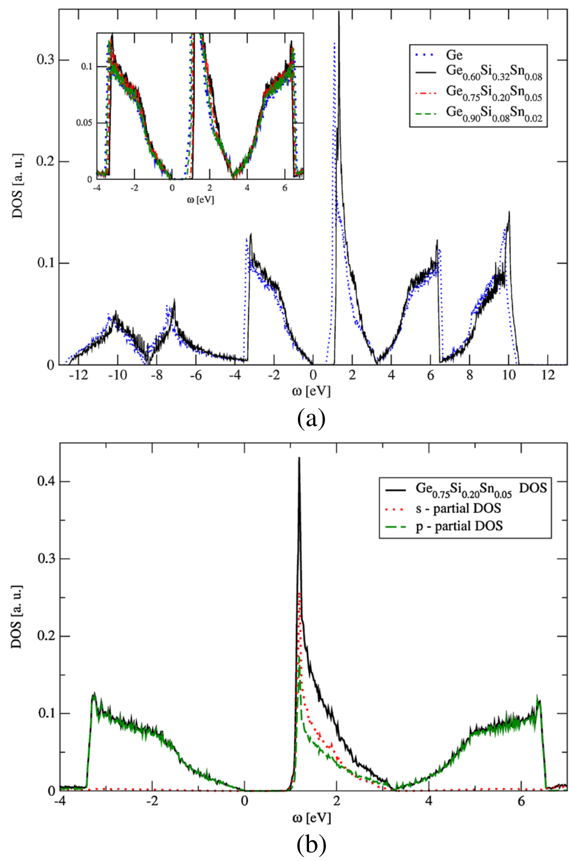

Figure 3. (a) Tight-binding and virtual crystal approximation total density of states for $Ge_{1-x-y}Si_xSn_y$ lattice matched to Ge (alloy compositions indicated in figure) compared with pure Ge DOS (dotted line). Inset: amplification around the gap. (b) Tight-binding and virtual crystal approximation total DOS (solid line) and partial densities of states (s-DOS: dotted line, p-DOS: dashed line) for $Ge_{0.75}Si_{0.20}Sn_{0.05}$.

the different alloy compositions: Z = 0.05, 0.08, 0.10, 0.15, 0.25, 0.30, 0.40, and 0.50, corresponding to the same samples experimentally studied in Refs. [8], [9]. Notice that the band structure changes smoothly and monotonously as a function of the alloy concentration Z. The energy of the maximum of the upper valence band, located at Γ, is seen to be practically independent of concentration. Moreover, as expected from the electronic structure of the two components of the "effective binary alloy", pure Ge and $Si_{0.79}Sn_{0.21}$ of Figure 1, for the relatively small Sn-concentrations shown in Figure 2, all ternary alloys formed also possess indirect band gaps. Whereas in general, the conduction band of the ternary alloy has four competing minima, located respectively at Γ, U (or$K$), L (as in pure Ge), and the minimum located near X (as in pure Si), only the latter two are seen to define the fundamental (indirect) gap for the ternary alloys depicted in Figure 2, which were experimentally studied in Refs. [8], [9]. In these cases, we found that the indirect gap is determined by the minimum of the conduction band at L for all Ge compositions $1 - Z \geq 0.674$ (with indirect gap values ranging from 0.758 eV at Z = 0.05 to 1.081 eV at Z = 0.326). Instead, it is interesting to notice that for smaller Ge compositions $Z > 0.326$, the relevant minimum of the conduction band, determining the indirect gap, has shifted to the Si-related one near X, whereas, for example, the indirect gap value obtained at $Z = 0.5$ is 1.092 eV. In connection with these results, it is interesting to mention that one of the final remarks of Ref. [8] was that future experimental and theoretical works should concentrate on determining the nature and energy of the indirect edges of these ternary alloys, being of outmost significance the elucidation of the conduction band structure, because of the indications for near overlap of various minima they found—as our electronic structure calculations now confirm.

In Figure 3(a), we show the total density of states (DOS) obtained in TB + VCA for the ternary alloy $Ge_{1-x-y}Si_xSn_y$

Prog. Photovolt: Res. Appl. 2015; **23**:112–118 © 2013 John Wiley & Sons, Ltd.
DOI: 10.1002/pip

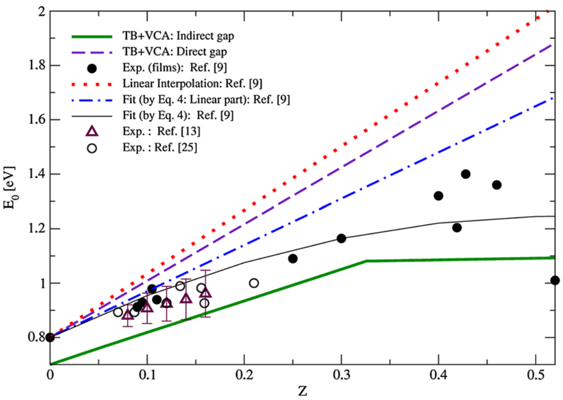

Figure 4. Compositional dependence of the band gap of $Ge_{1-Z}(Si_{0.79}Sn_{0.21})_Z$, matched alloys. Present (Tight-binding and virtual crystal approximation) results: indirect gap (thick solid line) and direct gap at Γ (dashed line). Other data included for comparison (experimental points and fits, from Refs. [9,13,25]: see text for details) correspond to the direct gap.

compared with pure Ge. The inset shows an amplification of the DOS in the energy range around the gap for several alloy compositions, which ensure the same alloy lattice parameter as in pure Ge [8,9]. The smooth dependence on composition is again observed here. In Figure 3(b), we show the total and partial densities of states obtained in TB + VCA for $Ge_{0.75}Si_{0.20}Sn_{0.05}$. The partial DOS shown corresponds to the projections of the total DOS onto the p and (s + s*) orbital subspaces of the TB basis. Notice that near the band gap, most of the DOS has *p* character, except for a peak in the *s*-partial DOS that is located just above the gap.

In Figure 4, we present our results respectively for the direct ($E_{0_{\mathrm{TB+VCA}}}$) and the indirect ($E_{I_{\mathrm{TB+VCA}}}$) band gaps of the ternary alloy $Ge_{1-Z}(Si_{0.79}Sn_{0.21})_Z$ lattice matched to Ge, as a function of the total doping Z into Ge. Our band gap results (in eV) can be fitted as follows:

$$E_{0_{\mathrm{TB+VCA}}}(Z) = 0.800 + 2.081\,Z \tag{2}$$

$$E_{I_{\mathrm{TB+VCA}}}(Z) = \begin{cases} 0.700 + 1.169\,Z & , Z \leq Z_C \\ 1.061 + 0.062\,Z & , Z > Z_C \end{cases} \tag{3}$$

where the indirect gap depends on a critical concentration: $Z_c = 0.326$, which in turn corresponds to respective critical concentrations: $x_c = 0.258$ of Si and $y_c = 0.068$ of Sn. It is clear that for the Ge lattice-matched ternary alloys studied, the fundamental gap is indeed predicted to be indirect in TB + VCA approximation, as previously mentioned in connection with Figure 2. Regarding their compositional dependence, the direct gap depends linearly on composition, as might be expected in this approximation, whereas the indirect gap clearly reflects the presence of two competing minima in the conduction band, with concentration $Z_C = 0.326$ dividing two different linear regimes. For compositions $Z \leq 0.326$, we find an indirect gap regime determined by the conduction band minimum at L (as in pure Ge), instead, for larger Z, the indirect gap is determined by the minimum located near X (related to Si). This can be compared with the behavior of binary $Ge_{1-x}Si_x$ alloys, where the indirect gap is known to change from Ge-like to Si-like at a critical Si-concentration of $x = 0.15$ [22]. Thus, we find that a small amount of Sn ($y_c = 0.068$) present in the ternary alloy has a profound effect on the indirect gap behavior modifying greatly ($x_c = 0.258$ in the ternary alloy vs. 0.15 in the binary) the critical Si-concentration at which the gap changes from Ge-like to Si-like.

For comparison with our TB + VCA results in Figure 4, we have also included three sets of recent experimental data, from which direct gap values of the ternary alloys lattice matched to Ge were obtained, which we shall discuss in the succeeding texts. The first set of experimental results for the direct gap included in Figure 4 was reported by D'Costa *et al.* in Refs. [8,9], who used room-temperature spectroscopic ellipsometry on ternary alloy films and who compared three different fits with their measured data. They find that their experimental results for the direct gap [9] are best described by a quadratic fit (thin solid line in Figure 4) obtained assuming that the compositional dependence of the direct band gap $E_0(Z)$ in the ternary alloy is quadratic (as a result of phenomenological mixed bowing effects[8,9]), namely:

$$E_0(Z) = E_0^{\mathrm{Ge}} + AZ + BZ^2 \tag{4}$$

where, $E_0^{Ge} = 0.80\,\mathrm{eV}$, $A = 1.70 \pm 0.42\,\mathrm{eV}$, and $B = -1.62 \pm 0.96\,\mathrm{eV}$ [9]. Figure 4 also shows the estimation of the direct gap of the ternary alloy made in Ref. [9], by linear interpolation (dotted line in Figure 4) between the known values of the direct gaps for pure Ge (0.8 eV), Si (4.1 eV), and α-Sn (–0.4eV) [23]. The increase of the band gap value as a function of the total (Si + Sn) concentration Z is mainly because of the larger value of the Si direct gap. Our TB + VCA results for the direct gap (dashed line in Figure 4) describe a linear dependence on Z but with a smaller positive slope (because of the difference discussed earlier between the direct gap values of $Si_{\beta}Sn_{1-\beta}$, which the TB + VCA and a simple linear interpolation predict) somewhat closer to the experimental data. Notice that the linear part of the quadratic fit of Equation (4) (dot-dashed line in Figure 4), has a still smaller slope, although it is not easy to infer what modifications in the TB + VCA approach might achieve a similar effect. It would be interesting to look into this problem in the light of the non-linearity recently reported for the compositional dependence of the lattice parameter in $Ge_{1-y}Sn_y$ binary alloys [24].

The second set of experimental results for the direct gap shown in Figure 4 was reported very recently by Beeler *et al.* in Ref. [13], who measured the optical responsivity of ternary alloy photodetectors grown on Ge. The five values of direct gap as a function of doping Z, (depicted by empty triangles in Figure 4) obtained for respective five devices, can be seen to lie slightly below the first set of experimental data discussed earlier [9], but agree with their quadratic fit within the experimental error bars [13].

The third and most recent set of experimental data on the direct gap of ternary alloys was obtained from high-performance near-infrared (IR) photodetectors produced with $Ge_{1-Z}(Si_\beta Sn_{1-\beta})_Z$ layers on Ge(100) by Chi Xu *et al*. [25]. The corresponding direct gap values appeared and are included in Figure 4, depicted by empty circles, and are seen to be also consistent within error bars with the experimental results [8,9,13] discussed earlier. In particular, Chi Xu *et al*. fitted their data[25] by the following:

$$E_0(x,y) = 0.803 + (1.86 \pm 0.34)\,x - (2.40 \pm 1.4)\,y \quad \text{(eV)}. \tag{5}$$

Lastly, comparing our gap results with the experimental data included in Figure 4 discussed earlier, we find that our TB + VCA prediction for the fundamental gap (i.e., the indirect gap, according to our calculations) lies close to the direct gap values obtained in films [9] and even closer to the gap values most recently reported in devices [13,25], especially if one takes into account the relatively large error bars for the experimental data and their fits (Equation (4) and Equation (5)). Although further experiments are needed to ascertain the true nature of the fundamental gap in these ternary alloys, the comparison of the experimental direct and TB + VCA fundamental gap data in Figure 4 is quite suggestive. Especially, considering the fact that there has been mention of experimental limitations making it difficult for a reliable identification of indirect and direct gaps in closely related compounds. Indeed, for binary $Ge_{1-y}Sn_y$ alloys, it was mentioned that the direct gap absorption could overlap with the indirect absorption edge [26,27], thus making it difficult for the determination of the critical Sn-concentration (y_c^*) for the indirect to direct gap crossover in these compounds. This may explain the large spread of values reported for y_c^* in the literature. Starting from Atwater *et al*. [27], whose optical absorption experiments predicted $0.11 < y_c^* < 0.15$, Ladrón de Guevara *et al.* [28] reported $0.10 < y_c^* < 0.13$ from transmittance measurements, D'Costa *et al.* [26] reported $y_c^* \sim 0.11$ with ellipsometry experiments, and recently Chen *et al.* [29] reported for the critical Sn-concentration $y_c^* \sim 0.07$ using photoluminescence. Theoretically, predictions for the critical Sn-concentration for the indirect to direct gap crossover in the binary $Ge_{1-y}Sn_y$ alloy yield y_c^*= 0.15 in TB + VCA [30], y_c^*= 0.17 with a charge self-consistent pseudo-potential plane wave method [31] and y_c^*= 0.11 with the empirical pseudopotential method with adjustable form factors fitted to experimental data [32], whereas with the full potential augmented plane wave plus local orbital method within density functional theory y_c^*= 0.105 [33].

Finally, we can also compare our TB + VCA predictions for the indirect gap with the value estimated by D'Costa it et al. in Ref. [8] for a ternary alloy sample not perfectly lattice matched to Ge, namely $Ge_{0.49}Si_{0.4}Sn_{0.11}$ (corresponding to: $Z = 0.51$ and $\beta = 0.785$). By modeling a $Ge/Ge_{0.49}Si_{0.4}Sn_{0.11}$ heterojunction using a combination of known and extrapolated or assumed parameters, including: band offsets, bowing parameters, and deformation potentials to describe strain effects, they estimated an indirect gap of 1.082 eV[8]. The latter value agrees well with the result we obtain with TB + VCA, yielding an indirect gap of 1.091 eV for $Ge_{0.49}Si_{0.4}Sn_{0.11}$.

Finally, we relax the condition of lattice matching to Ge and focus on the electronic and lattice structure of $Ge_{1-x-y}Si_xSn_y$ ternary alloys, which may exhibit the transition from indirect gap to direct gap as a function of concentration. Starting from the binary $Ge_{0.75}Sn_{0.25}$ alloy, with a direct gap in TB + VCA [30], we will now study ternary alloys with similar concentrations. We introduced three parameters to characterize the alloys at this stage:

(i) $\Delta = E_{min}(\vec{k} = \Gamma) - E_{min}(\vec{k} = L)$, which measures the energy difference between the two competing minima (Γ and L) of the conduction band, at this Ge concentration range: a negative value ($\Delta < 0$) indicates that the gap is direct, whereas $\Delta > 0$ indicates an indirect gap.

(ii) $\Delta_1^a = \frac{\Delta a}{a_{Ge}} = \frac{a(x,y) - a_{Ge}}{a_{Ge}}$: a parameter which measures the expansion (or contraction, if negative) of the alloy lattice with respect to pure Ge.

(iii) $\Delta_2^a = \frac{\Delta a}{a_{Ge_{1-y}Sn_y}} = \frac{a(x,y) - a_{Ge_{1-y}Sn_y}}{a_{Ge_{1-y}Sn_y}}$: a parameter which measures the expansion (or contraction, if negative) of the ternary alloy lattice with respect to the lattice parameter of binary $Ge_{1-y}Sn_y$ ($a_{Ge_{1-y}Sn_y}$).

In Figure 5, we show the results obtained for alloys with the same (75%) Ge content, smooth changes in the band-structure are observed as a function of concentration, as in all previous cases. Nevertheless, a crossover from the direct gap in the binary $Ge_{0.75}Sn_{0.25}$ alloy to an indirect gap in the ternary alloy is obtained as 1% of Sn is replaced

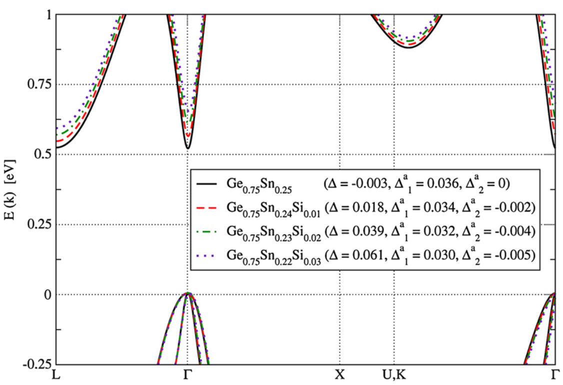

Figure 5. Tight-binding and virtual crystal approximation electronic structure of $Ge_{1-x-y}Si_xSn_y$ alloys with fixed Ge content: x + y = 0.25 . Refer to inset for detailed alloy concentrations and a table indicating corresponding values for the following parameters: Δ (sign indicates nature of gap: $\Delta < 0$: direct gap; $\Delta > 0$: indirect gap), and the lattice expansion coefficients: Δ_1^a and Δ_2^a, defined in the text.

Table I. Delta and lattice expansion coefficients for $Ge_{1-x-y}Si_xSn_y$ alloys with fixed Sn content.

$y = 0.25$ alloys	Δ (eV)	Δ_1^a	Δ_2^a
$Ge_{0.75}Sn_{0.25}$	-0.003	0.0358	0
$Ge_{0.74}Sn_{0.25}Si_{0.01}$	0.010	0.0355	-0.0004
$Ge_{0.73}Sn_{0.25}Si_{0.02}$	0.024	0.0351	-0.0008
$Ge_{0.72}Sn_{0.25}Si_{0.03}$	0.034	0.0347	-0.0011

Table II. Delta and lattice expansion coefficients for $Ge_{1-x-y}Si_xSn_y$ alloys with fixed Si content.

$x = 0.01$ alloys	Δ (eV)	Δ_1^a	Δ_2^a
$Ge_{0.75}Sn_{0.24}Si_{0.01}$	0.018	0.0340	0
$Ge_{0.74}Sn_{0.25}Si_{0.01}$	0.010	0.0350	0.0010
$Ge_{0.73}Sn_{0.26}Si_{0.01}$	0.003	0.0370	0.0030
$Ge_{0.72}Sn_{0.27}Si_{0.01}$	-0.005	0.0380	0.0040

by Si. The replacement of Sn by Si is also accompanied by a reduction of the alloy lattice parameter because of the difference ($r_{Si} < r_{Ge} < r_{Sn}$) in atomic radii [20], for all ternary alloys included in Figure 5, an expansion of the lattice is obtained with respect to pure Ge, whereas a contraction is obtained with respect to the binary alloy.

Similar trends are observed analizing the results for the ternary alloys with fixed Sn content ($y = 0.25$) included in Table I, or with fixed Si content ($x = 0.01$) included in Table II. Notice in Table II, that even in the presence of Si in a ternary alloy with an indirect gap, a direct gap is attainable if sufficient Sn is introduced to replace Ge.

In summary, we calculated the electronic structure of $Ge_{1-x-y}Si_xSn_y$ extending TB + VCA [14] to describe these ternary alloys. We analized the gap as a function of concentration for the ranges of most interest for technological applications [4,8], that is, $Ge_{1-Z}(Si_\beta Sn_{1-\beta})_Z$ ternary alloys lattice matched to Ge ($\beta = 0.79$). We found that the fundamental gap is indirect, taking values between 0.7 and 1.1 eV for $Z \leq 0.5$, thus confirming previous expectations, and close to the indications of optical measurements (ellipsometry) [8,9], and very recent experiments on new devices, ternary alloy-based photodetectors [13,25], for the direct gap. The competition of two minima in the conduction band is clearly distinguishable in the compositional dependence of the fundamental indirect gap dominating the pure Ge-related minimum at L for $Z \leq 0.326$ and the Si-related minimum near X for larger Z. Because no previous electronic structure calculations or experiments had thrown light on the fundamental indirect gap of these ternary alloys, we believe that our work represents a useful contribution in this rapidly advancing and active field, which will prompt new experiments to reliably identify the indirect and direct band gaps. Our results provide support to previous suggestions indicating that these ternary alloys would be suitable (fourth) components to integrate the multijunction heterostructures envisaged for high-efficiency solar cells for satellites, allowing to optimize the absorption frequency range [1,4,8,9].

Cecilia I. Ventura and Javier D. Fuhr are Investigadores Científicos del Consejo Nacional de Investigaciones Científicas y Técnicas (CONICET), Argentina. Cecilia I. Ventura acknowledges support from CONICET (PIP 0702) and ANPCyT (PICT 38357; PICT Redes 1776) and Rafael A. Barrio from CONACyT project 179616.

REFERENCES

1. D'Costa, VR, Cook, C, Menéndez, J, Tolle, J, Kouvetakis, J, Zollner, S. Transferability of optical bowing parameters between binary and ternary group-IV alloys. *Solid State Communications* 2006; **138**: 309–313.
2. Bett, AW, Dimroth, F, Stollwerck, G, Sulima, OV. III-V compounds for solar cell applications. *Appl. Phys. A* 1999; **69**: 119–129.
3. Vurgaftman, I, Meyer, JR, Ram-Mohan, LR. Band parameters for III-V compound semiconductors and their alloys. *J. Appl. Phys.* 2001; **89**: 5815 –5875.
4. Geisz, JF, Friedman, DJ. III-N-V semiconductors for solar photovoltaic applications. *Semicond. Sci. Technol.* 2002; **17**: 769–777, Dimroth F., Kurtz S., High-efficiency multijunction solar cells, *MRS Bull*, 2007; **32**: 230–235.
5. Recently, 43.5% efficiency has been reported for a new triple junction metamorphic solar cell. [Optics.org(2011-04-19)].
6. Soref, RA, Perry, CH. Optical band gap of the ternary semiconductor $Si_{1-x-y}Ge_xC_y$. *J. Appl. Phys* 1991; **70**: 2470–2473.
7. Aella P, Cook C, Tolle J, Zollner S, Chizmeshya AVG, Kouvetakis J. Optical and structural properties of $Si_xSn_yGe_{1-x-y}$ alloys. *Appl. Phys. Lett.* 2004; **84**: 888–890.
8. D'Costa, VR, Fang, YY, Tolle, J, Kouvetakis, J, Menéndez, J. Ternary GeSiSn alloys: new opportunities for strain and band gap engineering using group-IV semiconductors. *Thin Solid Films* 2010; **518**: 2531–2537.
9. D'Costa VR, Fang YY, Tolle J, Kouvetakis J, Menéndez J. Tunable optical gap at a fixed lattice constant in group-IV semiconductor alloys. *Phys. Rev. Lett.* 2009; **102**: 107403–1–4.
10. Bauer, M, Ritter, C, Crozier, PA, Ren, J, Menendez, J, Wolf, G, Kouvetakis, J. Synthesis of ternary SiGeSn semiconductors on Si(100) via Sn_xGe_{1-x} buffer layers. *Appl. Phys. Lett.* 2003; **83**: 2163–2165.
11. Mattila T, Wei SH, Zunger A. Localization and anticrossing of electron levels in $GaAs_{1-x}N_x$ alloys. *Phys. Rev. B* 1999; **60**: R11 245–R11 248.

12. Beeler, RT, Smith, DJ, Kouvetakis J, Menéndez, J. GeSiSn photodiodes with 1eV optical gaps grown on Si(100) and Ge(100) platforms. *IEEE Journal of Photovoltaics* 2012; **2**: 434–440.
13. Beeler, R.T, Xu, C, Smith, DJ, Grzybowski, G, MÃľnendez J, Kouvetakis, J. Compositional dependence of the absorption edge and dark currents in $Ge_{1-x-y}Si_xSn_y$/Ge(100) photodetectors grown via ultra-low-temperature epitaxy of Ge_1H_{10}, Si_4H_{10}, and SnD_4. *Appl. Phys. Lett.* 2012; **101**: 221111.
14. Jenkins DW, Dow JD. Electronic properties of metastable Ge_xSn_{1-x} alloys. *Phys. Rev. B* 1987; **36**: 7994–8000.
15. Jaros, M. Electronic properties of semiconductor alloy systems. *Rep. Prog. Phys.* 1985; **48**: 1091–1154.
16. Newman KE, Dow JD. Theory of deep impurities in silicon-germanium alloys. *Phys. Rev. B* 1984; **30**: 1929–1936.
17. Nordheim, L. Zur Elektronentheorie der Metalle. *Ann. Phys (Leipzig)* 1931; **401**: 607–640.
18. Chadi DJ. Spin-orbit splitting in crystalline and compositionally disordered semiconductors. *Phys. Rev. B* 1977; **16**: 790–796.
19. Vogl, P, Hjalmarson, HP, Dow, JD. A semiempirical tight-binding theory of the electronic structure of semiconductors. *J. Phys. Chem. Solids* 1983; **44**: 365–378.
20. Madelung, O. *Semiconductors - Basic Data*. Springer: Berlin, 1996.
21. Vegard, L. Die konstitution der mischkristalle und die raumfuellung der atome. *Zeitschrift fuer Physik* 1921; **5**: 17–26.
22. Weber, L, Alonso, MI. Near-band-gap photoluminescence of Si-Ge alloys. *Phys. Rev. B* 1989; **40**: 5683–5693.
23. Adachi S. *Properties of Group-IV, III-V and II-VI Semiconductors*. John Wiley & Sons: Hoboken, N.J., 2005.
24. Beeler R, Roucka R, Chizmeshya AVG, Kouvetakis J, Menéndez J. Nonlinear structure-composition relationships in the $Ge_{1-y}Sn_y$/Si(100) (y<0.15) system. *Phys. Rev. B* 2011; **84**: 035204-1-8.
25. Xu, C, Beeler, T, Grzybowski, GJ, Chizmeshya, AVG, et. al. Molecular synthesis of high-performance near-IR photodetectors with indepedently tunable structural and optical properties based in Si-Ge-Sn. *J. Am. Chem. Soc.* 2012; **134**: 20756.
26. D'Costa, VR, Cook, CS, Birdwell, AG, Littler, CL, Canonico, M, Zollner, S, Kouvetakis, J, Menendez, J. Optical critical points of thin-film $Ge_{1-y}Sn_y$ alloys: a comparative $Ge_{1-y}Sn_y$/$Ge_{1-x}Si_x$ study. *Phys. Rev. B* 2006; **73**: 125207.
27. He, Gang, Atwater, Harry A. Interband transitions in Sn_xGe_{1-x} alloys. *Phys. Rev. Lett.* 1997; **79**: 1937.
28. Pérez Ladrón de Guevara, H. et al. Determination of the optical energy gap of $Ge_{1-x}Sn_x$ alloys with 0¡x¡0.14. *Appl. Phys. Lett.* 2004; **84**: 4532, H. Pérez Ladrón de Guevara, A. G. Rodríquez, H. Navarro-Contreras, Nonlinear behavior of the energy gap in $Ge_{1-x}Sn_x$ alloys at 4 K, *Appl. Phys. Lett.*, 2007; **91**:161909.
29. Chen, R, Lin, H, Huo, Y, Hitzman, C, Kamins, T, Harris, JS. Increased photoluminescence of strain-reduced, high-Sn composition $Ge_{1-x}Sn_x$ alloys grown by molecular beam epitaxy. *Appl. Phys. Lett.* 2011; **99**: 181125.
30. Ventura, CI, Fuhr, JD, Barrio, RA, Non-substitutional single-atom defects in the $Ge_{1-x}Sn_x$ alloy. *Phys. Rev. B* 2009; **79**: 155202–1/12.
31. Moontragoon, P, Ikonic, Z, Harrison, P. Band structure calculations of Si-Ge-Sn alloys: achieving direct band gap materials. *Semiconductor Science and Technology* 2007; **22**: 742–748.
32. Lu Low K, Yang Y, Han G, Fan W, Yeo Y. Electronic band structure and effective mass parameters of $Ge_{1-x}Sn_x$. alloys. *J. Appl. Phys.* 2012; **112**: 103715–1–9.
33. Chibane, Y. Ferhat M. electronic structure of Sn_xGe_{1-x} alloys for small Sn compositions: unusual structural and electronic properties. *J. Appl. Phys.* 2010; **107**: 053512.

 Prog. Photovolt: Res. Appl. 2015; **23**:112–118
DOI: 10.1002/pip